Supporting Information for

Novel Multi-Functional Iron Chelators of the Aroyl Nicotinoyl Hydrazone Class that Markedly Enhance Cellular NAD^+/NADH Ratios

Zhixuan Wu[†], Duraippandi Palanimuthu[†], Nady Braidy[§], Nor Hawani Salikin[Φ], Suhelen Egan[Φ], Michael L. H. Huang[†] and Des R. Richardson[†γ*]

[†]*Molecular Pharmacology and Pathology Program, Department of Pathology and Bosch Institute, The University of Sydney, Sydney, New South Wales, 2006, Australia.*

[§]*Centre for Healthy Brain Ageing, School of Psychiatry, University of New South Wales, Sydney, 2031, Australia.*

[Φ]*School of Biological, Earth and Environmental Sciences, Centre for Marine Science and Innovation, University of New South Wales, Sydney, 2031, Australia.*

[γ]*Department of Pathology and Biological Responses, Nagoya University Graduate School of Medicine, 65 Tsurumai, Showa-ku, Nagoya 466-8550, Japan.*

***Corresponding author:** Dr. Des R. Richardson; Molecular Pharmacology and Pathology Program, Discipline of Pathology, Medical Foundation Building (K25), The University of Sydney, Sydney, New South Wales 2006, Australia. Tel.: + 61 2 9036-3026; Email: d.richardson@med.usyd.edu.au

X-ray Diffraction

Methods

Single crystals of SNH2 and SNH6 were isolated from methanol and their single-crystal X-ray diffraction data were collected at 150 K on a Rigaku Oxford Diffraction SuperNova diffractometer equipped with an Atlas CCD detector and Cu-Kα radiation (1.54184 Å). Data reduction, cell refinements and empirical absorption (multiscan) corrections were carried out using Oxford Diffraction CrysAlisPro Software. The structures were solved using direct methods either with SIR92 or with SHELX-86 and refined further by full matrix least-squares on F^2 using SHELXL-2014/7 (Farrugia, 1999; Sheldrick, 2008). All non-hydrogen atoms were anisotropically refined and the hydrogen atoms were either located or fixed using a riding model. Molecular structure diagrams depicted in **Figure S1** were generated with ORTEP-3. Crystal data have been deposited with the Cambridge Crystallographic Data Centre (CCDC numbers: 1878972 and 1878975 for SNH2 and SNH6, respectively).

Results and Discussion

The molecular structure of the ligands, SNH2 and SNH6, were determined by single crystal X-ray crystallography (**Fig. S1**). The ligand, SNH2, crystallised as a dimer and two water molecules were present, where one water molecule strongly hydrogen bonded with two ligands. Similarly, SNH6 was stabilised by intra- and inter-molecular hydrogen bonds, as well as hydrogen bonding with a water molecule. Indeed, one water molecule was strongly hydrogen bonded with three SNH6 molecules; first with the nicotinyl nitrogen (O4−H15A…N3 distance 2.02 Å), second with the amide C=O (O4−H15A…O3 distance 1.96 Å) and third with the amide NH (N2−H8…O4 distance 2.03 Å). Moderate intra-molecular hydrogen bonding between the salicylyl oxygen and hydrazone NH (N2-H8…O1 distance 2.74 Å) was present. An intra-molecular hydrogen bond between the salicylyl OH proton and the imine nitrogen was also observed (O1−H1…N1 distance 2.58 Å).

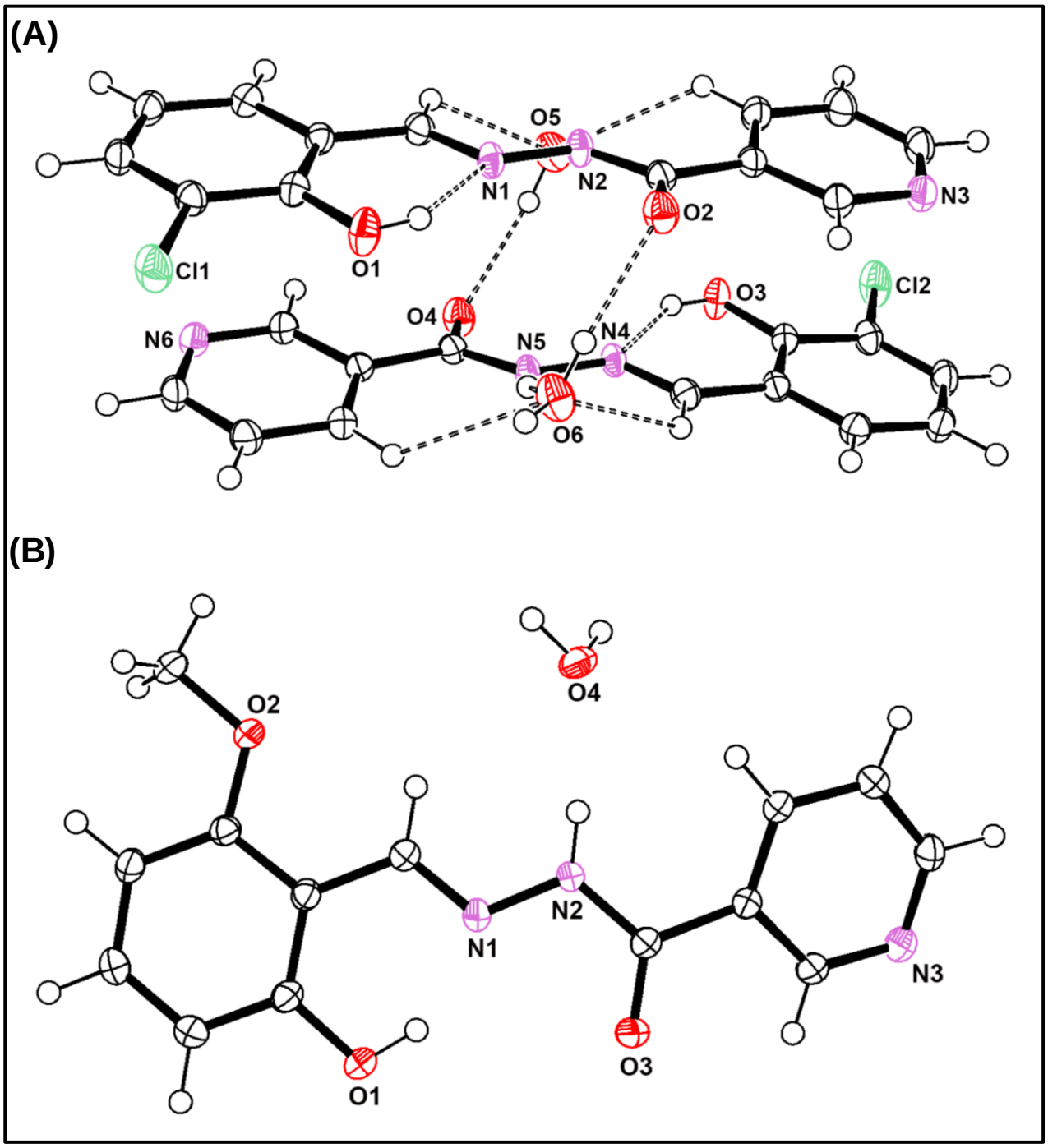

Figure S1. ORTEP diagrams of the single crystal X-ray structures of (A) SNH2 and (B) SNH6 drawn at 50% probability level.

General Procedure for the Preparation of Iron Complexes

The Fe complexes of the ONO-donor ligands, SNH6, SNH8, and PrNH1, were synthesised according to a previously reported procedure (Palanimuthu *et al.*, 2017). Briefly, to the ligand (0.5 mmol) dissolved in ethanol (10 mL), ferric perchlorate hexahydrate (115 mg, 0.25 mmol) was added, leading to a dramatic color change, which indicated complex formation. After 60 min of refluxing, a precipitate formed was filtered, washed with ethanol, and dried in a vacuum desiccator.

The Fe complex of the NNO-donor, PCNH, was prepared by following an alternative procedure because of the preference of pyridine-derived hydrazones to form Fe^{II} complexes (Bernhardt *et al.*, 2007). Accordingly, PCNH (0.135 mg, 0.5 mmol) was dissolved in acetonitrile (15 mL) and excess triethylamine (10 mmol) and the solution degassed under nitrogen. A solution of ferrous perchlorate hexahydrate (93 mg, 0.25 mmol) in degassed acetonitrile (5 mL) was added to the ligand solution under reflux. A colour change from colorless to green was observed. After 3 h, the precipitate formed was collected by filtration, washed with acetonitrile and dried in a vacuum desiccator.

$[Fe(PCNH\text{-}H)_2]\cdot 3H_2O$

Green solid (0.18 g). Yield: 41%. ESI-MS (positive mode) in CH_3OH: found mass: 529.086 (100%), Calc. mass for $FeC_{24}H_{18}N_8O_2Na$: 529.08 $[M+Na^+]^+$. Anal. Calc. $FeC_{24}H_{18}N_8O_2\cdot 3H_2O$ (%): C 51.44, H 4.32, N 20.00. Found (%): C 51.84, H 4.00, N 19.70. IR (cm^{-1}) 1582 (m), 1488 (m), 1459 (s), 1314 (m), 1292 (m), 1150 (s), 1065 (m), 1022 (m), 923 (m), 719 (m), 671 (m), 522 (m), 437 (m).

[Fe(SNH6-H)$_2$]ClO$_4$

Black solid (0.20 g). Yield: 51%. ESI-MS (negative mode) in CH_3OH: found mass: 594.02 (100%), Calc. mass for $FeC_{28}H_{22}N_6O_6$: 594.10 $[M-2H^+-ClO_4^-]^-$. Anal. Calc. for $FeC_{36}H_{44}N_6O_8Cl\cdot0.5H_2O$ (%): C 54.80, H 5.75, N 10.65. Found (%): C 54.76, H 5.96, N 10.42. IR (cm^{-1}) 3039 (w), 1593 (s), 1549 (s), 1525 (m), 1459 (s), 1434 (s), 1380 (m), 1340 (m), 1253 (s), 1156 (w), 1103 (vs, ClO_4^-), 1077 (s), 1048 (s), 788 (s), 718 (s), 619 (m), 592 (m), 556 (m), 475 (m), 433 (m).

[Fe(SNH8-H)$_2$]ClO$_4$

Dark green solid (0.22 g). Yield: 50%. ESI-MS (negative mode) in CH_3OH: found mass: 727.83 (100%), Calc. mass for $FeC_{26}H_{14}Br_2F_2N_6O_4$: 727.87 $[M-2H^+-ClO_4^-]^-$. Anal. Calc. for $FeC_{26}H_{16}Br_2ClF_2N_6O_8$ (%): C 37.65, H 1.94, N 10.13. Found (%): C 37.67, H 2.08, N 9.93. IR (cm^{-1}) 3063 (w), 2116 (w), 1601 (s), 1542 (s), 1433 (s), 1351 (m), 1300 (m), 1234 (s), 1207 (m), 1085 (vs, ClO_4^-), 1025 (s), 919 (w), 821 (m), 778 (m), 717 (s), 675 (s), 613 (s), 523 (m), 422 (vs).

[Fe(PrNH1-H)(PrNH1-H$_2$)]

Black solid (0.20 g). Yield: 51%. ESI-MS (negative mode) in CH_3OH: found mass: 747.95 (100%), Calc. mass for $FeC_{30}H_{24}Br_2N_6O_4$: 747.96 $[M-H^+]^-$. Anal. Calc. for $FeC_{30}H_{25}Br_2N_6O_4$ (%): C 48.09, H 3.36, N 11.22. Found (%): C 48.25, H 3.31, N 11.08. IR (cm^{-1}) 3067 (w), 2970 (w), 2870 (w), 1562 (s), 1531 (s), 1467 (s), 1396 (s), 1315 (s), 1253 (m), 1215 (m), 1163 (m), 1134 (m), 1045 (m), 1022 (m), 931 (m), 817 (s), 754 (m), 724 (s), 648 (s), 533 (m), 450 (s).

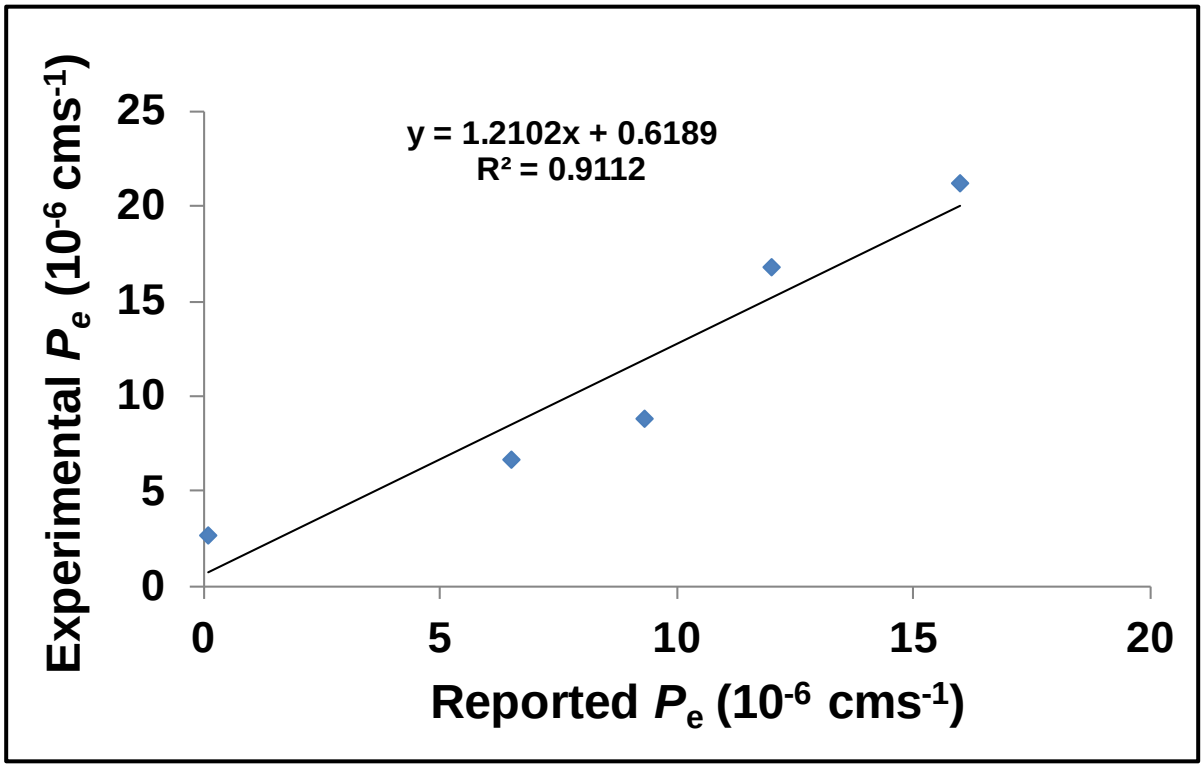

Figure S2. The linear correlation between experimental and reported permeability values of five commercial drugs, namely Theophylline, Verapamil, Progesterone, Chlorpromazine, and Donepezil, obtained by the PAMPA-BBB assay.

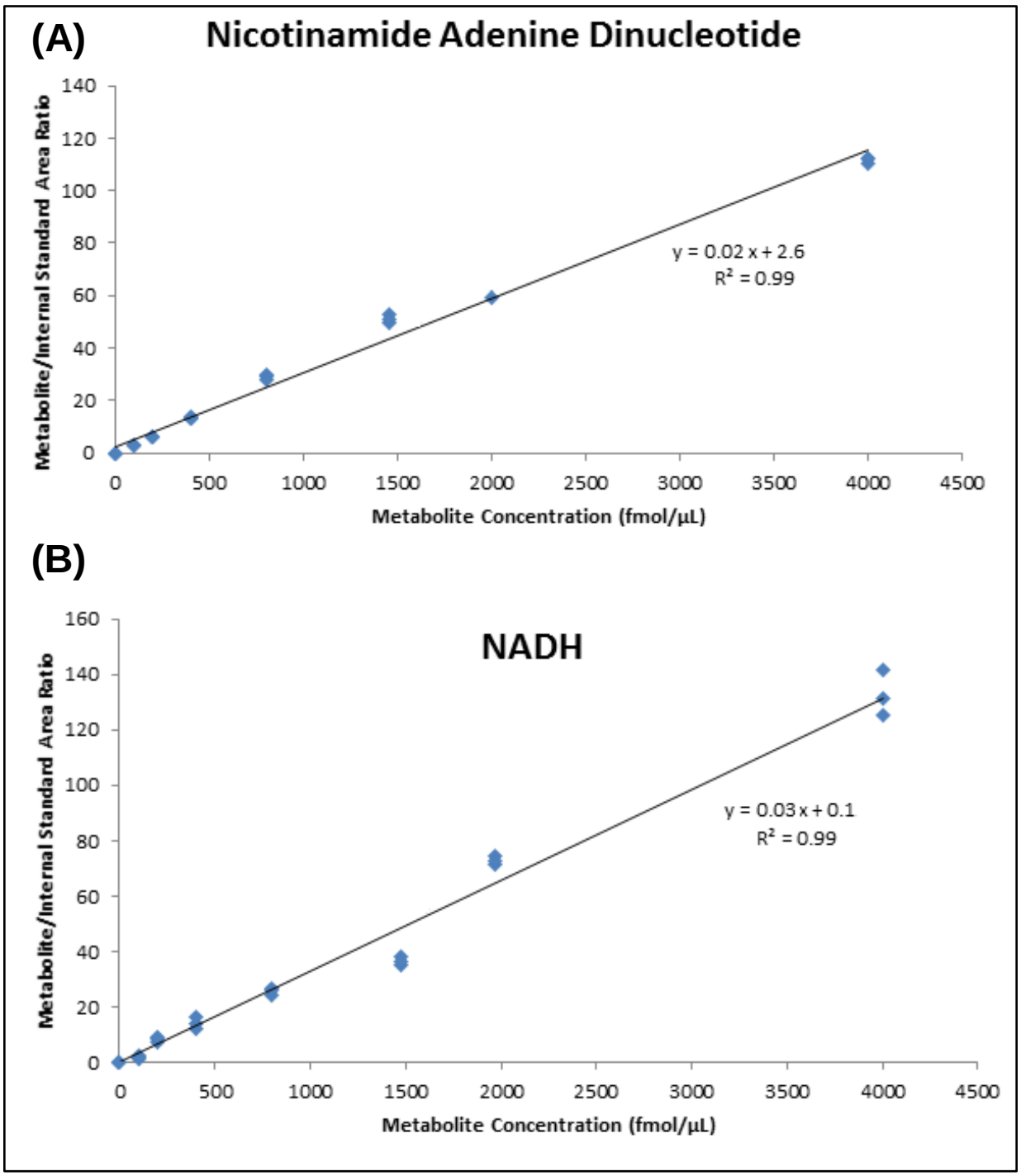

Figure S3. Individual standard curves for **(A)** NAD^+ and **(B)** NADH using LC-MS.

Table S1. Prediction of CNS penetration based on ranges of permeability values of PAMPA-BBB assay determined in **Figure S2** and as suggested by Di *et al.* (P_e, 10^{-6} cm.s^{-1}; Di *et al.*, 2003).

Compounds of high BBB permeation (CNS+)	$P_e > 5.459$
Compounds of potential BBB permeation (CNS+/-)	$5.459 > P_e > 3.039$
Compounds of low BBB permeation (CNS-)	$P_e < 3.039$

Table S2. Retention times and MS/MS transitions used for NAD^+ and NADH.

Analyte	Retention time (minutes)	Polarity	Transitions (*m/z*)	Collision Energy (V)
NAD	6.65	+	664.000>428, 524	18
NADH	10.70	+	666.200>514, 649	20
$^2H_4$-NAM	2.36	+	127.30>80	25

References

Bernhardt PV, Chin P, Sharpe PC, & Richardson DR. (2007). Hydrazone chelators for the treatment of iron overload disorders: iron coordination chemistry and biological activity. Dalton Transactions, (30), 3232-3244.

Di L, Kerns EH, Fan K, McConnell OJ, & Carter GT. (2003). High throughput artificial membrane permeability assay for blood-brain barrier. European Journal of Medicinal Chemistry, 38(3), 223-232.

Farrugia LJ. (1999). WinGX suite for small-molecule single-crystal cystallography. Journal of Applied Crystallography, 32(4), 837-838.

Palanimuthu D, Poon R, Sahni S, Anjum R, Hibbs D, Lin HY, *et al.* (2017). Novel class of thiosemicarbazones show multi-functional activity for the treatment of Alzheimer's disease. European Journal of Medicinal Chemistry, 139, 612-632.

Sheldrick GM. (2008). A short history of SHELX. Acta Crystallographica A, 64(1), 112-122.